Accelerated Algorithm for The Classical SIRT Method in CT Image Reconstruction

Jian Dong
Tianjin Key Laboratory of Information Sensing & Intelligent Control, Tianjin University of Technology and Education,
Hexi District, Tianjin 300222, China
dongjian2007.happy@163.com

Hiroyuki Kudo
Faculty of Engineering, Information and Systems, University of Tsukuba
Tennoudai 1-1-1, Tsukuba
305-8573, Japan
kudo@cs.tsukuba.ac.jp

Yongchae Kim
Graduate school of Systems and Information Engineering, University of Tsukuba
Tennoudai 1-1-1, Tsukuba
305-8573, Japan
acevip12@hotmail.com

ABSTRACT
In this paper, we developed an accelerated algorithm for the classical simultaneous iterative reconstruction technique (SIRT) method applied in CT image reconstruction. The proposed algorithm possesses the following two features. First, it can flexibly handle the image reconstruction problem where projection data is contaminated by Poisson noise. This property makes it successful in compensating the disadvantage of the typical algebraic reconstruction technique (ART) method. Second, we utilize Passty's proximal splitting framework to construct a row-action type accelerated iterative algorithm to minimize the cost function. The accelerating strategy makes it successful in compensating the disadvantage of the famous SIRT method. We proved that the new algorithm can achieve significant image quality with noise reduction in less than 10 iterations, while SIRT needs more than 200 iterations. Both digital phantom and clinical abdominal CT image were reconstructed for demonstrating the efficiency of the proposed method.

CCS Concepts
•Applied computing→Life and medical sciences→Computational biology→Imaging

Keywords
Computed Tomography; Image Reconstruction; Acceleration; ART; SIRT; Proximal Splitting; Algorithm Development.

1. INTRODUCTION
X-ray computed tomography (CT) has become the indispensable means of medical imaging examination. CT image reconstruction deals with the inverse problem that solves a transaxial slice image of body part from the measured projection data (sinogram) [1]. The reconstruction algorithms can generally be divided into two groups which are analytical methods and iterative methods. Filtered back-projection (FBP) method is exactly a typical representative of analytical methods [2]. The famous algebraic reconstruction technique (ART) method and simultaneous iterative reconstruction technique (SIRT) method are the classical algorithms in the iterative reconstruction categories [3-4]. Along with the improving computing ability of computers, the iterative algorithms have revealed superiority than the analytical ones in terms of the following aspects. First, the iterative algorithms can handle some image quality degradation factors during the reconstructing process, such as beam hardening or partial volume effect. But the analytical tools are not mature enough to transform the degradation factors as some special line integral models. Second, the cost functions of iterative algorithms can be designed to take some statistical properties of noise into account. Thus the iterative methods are more powerful in reducing noise of the reconstructed images than the analytical methods. Third, in the case of a limited view or sparse view of projection data, the analytical methods will lead to heavy streak artifacts in reconstructed images. But the iterative algorithms can avoid such artifacts by adding a regularization term in cost function [5].

Even though the iterative algorithms are widely used in the task of CT image reconstruction, the classical ART and SIRT algorithm even possess some disadvantages in the ability of reducing noise or convergence speed. ART method was proposed in early 1970s for image reconstruction of electron microscope. The solution is determined by iterative projection operations to hyperplanes. In this process, only one factor of measured projection data is used to achieve one image update, which successfully make the algorithm be an efficient row-action type one. The convergence speed of ART method is desirable. However, when the projection data is contaminated by Poisson noise, hyperplanes will no longer intersect at one point. As the iteration goes on, it pushes the unknown solution to fall into periodic solutions which is called limit cycle. Therefore, the ART algorithm is still defective in removing statistical noise in the task of image reconstruction. On the other hand, the SIRT method will averagely project to all the hyperplanes, and has the potential to select the averaged direction for the next solution modification. Thus it is outstanding in reducing statistical noise in reconstruction. However, the SIRT method will use all the factors of measured projection data in one image update, which exactly causes its low convergence speed [6]. Overall, an updating algorithm with the properties of both high convergence speed and reducing statistical noise ability is strongly needed by the image reconstruction community.

In recent years, researchers explored some accelerating methods for image reconstruction algorithms, some of which are based on massively parallel graphics processing units (GPU) cores. These

ICMIP 2020, January 10 – 12, 2020, Nanjing, China

ACM ISBN 978-1-4503-7664-8/20/01…$15.00
https://doi.org/10.1145/3381271.3381275

attempts successfully guaranteed 3D image reconstructions within reasonable execution times [7]. However, these methods only distribute computational loads to parallel calculations instead of reducing computing cost. Dong et al. proposed an accelerated algorithm for sparse-view CT image reconstruction by using alternating direction method of multipliers (ADMM) and achieved promising results [8]. Nowadays, image reconstruction methods using deep learning have been actively investigated [9-10]. But there does not yet exist a clear evidence which proves that they outperform advanced compressed sensing techniques.

In this paper, we proposed an accelerated algorithm for the classical SIRT method. The new algorithm not only inherited the SIRT's characteristic of reducing statistical noise, but also equipped with a row-action type structure like the ART method. To minimize the least-squares cost function, we introduced proximal splitting strategy based on Passty's framework to constructed an accelerated iterative algorithm [11]. In the proximal splitting of Passty's framework, creating the more sub-functions by dividing cost function, the better convergence performance will happen. Thus, we divided cost function extremely in small lots and then applied the proximity operator to each sub-function. The proposed algorithm converged quickly to the exact minimizer. Furthermore, we designed a projection data subset-independent step-size controller which ideally controls the noise propagation from projection data to the reconstructed image. We proved that the new algorithm can achieve significant image quality with noise depression in less than 10 iterations, while SIRT needs more than 200 iterations. Numerical chest phantom and clinical abdominal CT image were reconstructed for demonstrating the efficiency of the proposed method.

2. ART AND SIRT ALGORITHM

2.1 ART

The aim of CT image reconstruction is to reconstruct an transaxial slice image from measured projection data. When iterative methods are used for image reconstruction, the problem can be formulated as solving a linear equation $\mathrm{A}\vec{x} = \vec{b}$, where $\vec{b} = (b_1, b_2, \cdots, b_I)^T$ denotes the measured projection data, $\vec{x} = (x_1, x_2, \cdots, x_J)^T$ represents the attenuation coefficients of object to be reconstructed, and $\mathrm{A} = \{a_{ij}\}$ is the $I \times J$ system matrix. For ART method, the solution is progressively obtained by making projecting operation to the $\vec{a}_i^T\vec{x} = b_i$ ($i = 1,2,\cdots I$) hyperplanes sequentially. Figure.1 demonstrates a simulated calculation procedures of ART algorithm, where I and J are assumed to be 2 for a simple explanation. The projecting operation from $\vec{x}^{(0)}$ to the hyperplane $\vec{a}_1^T\vec{x} = b_1$ guarantees the next iterative $\vec{x}^{(1)}$ to satisfy both $\vec{a}_1^T\vec{x} = b_1$ and the minimization of $\left\|\vec{x} - \vec{x}^{(0)}\right\|^2$.

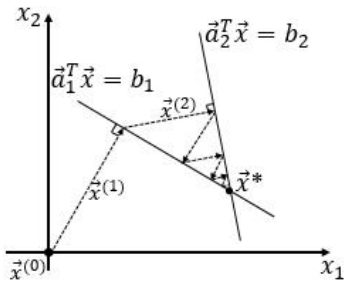

Figure 1. Simulated calculation procedures of ART algorithm when *I*=2, *J*=2.

The ART algorithm can be achieved based on the following steps:
Step 1: Initialization of $\vec{x}^{(0)} \leftarrow 0$.
Step 2: Iteration by the following formula when k =0,1,2, ⋯.

$$\vec{x}^{(k+1)} = \vec{x}^{(k)} + \frac{b_i - \vec{a}_i^T\vec{x}^{(k)}}{\|\vec{a}_i\|_2^2}\vec{a}_i \quad (1)$$

where $\vec{a}_i$ corresponds to the i-th row of the system matrix A, and the expression like $\|\vec{p}\|_2^2$ is defined as $\|\vec{p}\|_2^2 = \sum_{t=1}^{T} p_t^2$.

During the iteration, only one factor of projection data b_i is used for one image update. This is the row-action type procedure which determines the high convergence speed of ART method. In the case of $I \geq J$, we furtherly discuss the situations with and without noises in the projection data. When there are not noises in projection data, the hyperplanes insect in one point which is exactly the right solution. When there are noises in projection data, due to the presence of noise, $\mathrm{A}\vec{x} = \vec{b}$ becomes contradictory without solutions. And this is the mechanism of ART unsuccessful in reconstructing an image from the noise contaminated projection data.

2.2 SIRT

The strategy of treating the noise contained task which is instructed in Section 2.1 is the SIRT algorithm. In this situation, SIRT is assigned to solve the following linear equation:

$$\mathrm{A}\vec{x} = \vec{b} + \vec{n} \quad (2)$$

where $\vec{n}$ denotes the statistical noise contained in projection data. To achieve the noise depression effect in the reconstruction procedure, it is a critical point that let the candidate solution subject to all the equations $\vec{a}_i^T\vec{x} = b_i + n_i$ ($i = 1,2,\cdots I$) averagely. Generally, a cost function in the form of least-squares (shown in Eq.3) is usually utilized by SIRT algorithm.

$$F(\vec{x}) = \left\|\mathrm{A}\vec{x} - \vec{b}\right\|^2 \quad (3)$$

A simple way to minimize $F(\vec{x})$ is to set $\partial F(\vec{x})/\partial\vec{x} = 0$, *i.e.* Eq. 4.

$$A^T\mathrm{A}\vec{x} = A^T\vec{b} \quad (4)$$

The most used iterative strategy for solving Eq. (4) is Landweber method [12]. Subsequently, The SIRT algorithm can be derived as the following steps:
Step 1: Initialization of $\vec{x}^{(0)} \leftarrow 0$.

Step 2: Iteration by the following formula when k =0,1,2, ⋯.

$$\vec{x}^{(k+1)} = \vec{x}^{(k)} - \alpha A^T(\mathrm{A}\vec{x}^{(k)} - \vec{b}) \quad (5)$$

where A^T denotes the back-projection procedure, and $\alpha > 0$ is step-size which is used to control the image update magnitude. It is necessary to set α as $0 < \alpha < 2/\|A^T\mathrm{A}\|$ as to guarantee the algorithm convergence. In SIRT algorithm, it is obvious that all the projection data factors of $\vec{b}$ are used in one image update, which restricts the convergence speed.

3. METHODS

3.1 Mathematical Tools

In this paper, we proposed an acceleration algorithm for the aforementioned SIRT algorithm. In order to minimize the cost function of Eq. (3), we used the proximal splitting technique. Before showing the process of minimizing $F(\vec{x})$, we first introduce two important mathematical tools which provide us the method for seeking the optimal solution.

[**Proximity Operator**] For a proper lower-semi-continuous convex function $J(\vec{x})$: $R^N \rightarrow \mathrm{R} \cup \{+\infty\}$ (possibly non-

differentiable), the proximity (*prox*) operator is defined as Eq. (6), where $\vec{z},\vec{x} \in R^N$, and $\gamma > 0$ is the step-size parameter.

$$prox_{\gamma J}(\vec{z}) = \arg min_{\vec{x} \in R^N} \left(J(\vec{x}) + \frac{1}{2\gamma} \|\vec{x} - \vec{z}\|^2 \right) \quad (6)$$

It is known that the fixed point satisfying $\vec{x} = prox_{\gamma J}(\vec{z})$ coincides with the minimizer of $J(\vec{x})$. It means that the iteration formula in the form of $\vec{x}^{(k+1)} = prox_{\gamma J}(\vec{x}^{(k)})$ necessarily converges to a minimizer of $J(\vec{x})$. Such an iterative algorithm is called the proximal minimization algorithm [11]. It is obvious that the iterative formula Eq. (5) can also be derived by this tool. In order to construct an accelerated implementation, we furtherly divide $J(\vec{x})$ into a series of sub-functions. And the principal called proximal splitting is followed.

[**Proximal Splitting**] Let us consider the convex minimization problem expressed in Eq. (7).

$$min_{\vec{x} \in R^N} J(\vec{x}) \equiv J_1(\vec{x}) + J_2(\vec{x}) + \cdots J_n(\vec{x}) \quad (7)$$

where $J_1(\vec{x})$, $J_2(\vec{x})$, $\cdots J_n(\vec{x})$ can possibly be non-differentiable convex functions from R^N to [-∞,+ ∞]. The proximal splitting is a framework for constructing an iterative algorithm to minimize $J(\vec{x})$ by sequentially calculating *prox* operator $\vec{x}^{(k,i+1)} = prox_{\gamma^{(k)} J_i}(\vec{x}^{(k,i)})$ on each $J_i(\vec{x})$ in ascending order $i = 1,2,\cdots n$. For a better minimization, it is known that the step-size parameter $r^{(k)} \rightarrow 0$ ($k \rightarrow \infty$ and k denotes the iteration number) should meet the conditions $\sum_{k=0}^{\infty} \gamma^{(k)} = \infty$, $\sum_{k=0}^{\infty} (\gamma^{(k)})^2 < \infty$.

3.2 Algorithm Derivation

Below, we explain the derivation of the accelerated implementation by using proximal splitting theory. We first split the cost function in Eq. (3) to sub-cost functions as Eq. (8).

$$F(\vec{x}) = \left\|A\vec{x} - \vec{b}\right\|^2 = \sum_{i=0}^{I} f_i(\vec{x}), \quad f_i(\vec{x}) = \left\|\vec{a}_i^T \vec{x} - b_i\right\|^2 \quad (8)$$

where I is the dimension of projection data. Therefore, each iteration of the accelerated algorithm proceeds by applying the *prox* operators corresponding to $f_1(\vec{x})$, $f_2(\vec{x})$, $\cdots f_I(\vec{x})$ successively. Therefore, the outline of the accelerating algorithm can be sketched below.

loop k=0, 1, 2, ⋯
  loop i=1, 2, ⋯, I
  $\vec{x}^{(k,i+1)} = prox_{\alpha^{(k)} f_i}(\vec{x}^{(k,i)})$
  $\vec{x}^{(k+1,1)} = \vec{x}^{(k,I+1)}$ (9)

where k denotes the main iteration number and i denotes the sub iteration number. The *prox* operator corresponding to $f_i(\vec{x})$ is expressed below.

$$\vec{x}^{(k,i+1)} = prox_{\alpha^{(k)} f_i}(\vec{x}^{(k,i)}) = \arg min_{\vec{x} \in R^N} \left(\left\|\vec{a}_i^T \vec{x} - b_i\right\|^2 + \frac{1}{2\alpha^{(k)}} \left\|\vec{x} - \vec{x}^{(k,i)}\right\|^2 \right) \quad (10)$$

where $\alpha^{(k)} > 0$ represents step-size of the k-th iteration. The optimization problem can be solved in closed form by using the standard Lagrange multiplier technique [13]. First, by introducing an additional variable y, the above minimization problem can be converted into the constrained minimization below.

$$\arg min_{(\vec{x},y)} \left(\|y - b_i\|^2 + \frac{1}{2\alpha^{(k)}} \left\|\vec{x} - \vec{x}^{(k,i)}\right\|^2 \right) s.t. \vec{a}_i^T \vec{x} = y \quad (11)$$

The Lagrangian function corresponding to Eq. (11) is defined by

$$L(\vec{x},y,\lambda) = \|y - b_i\|^2 + \frac{1}{2\alpha^{(k)}} \left\|\vec{x} - \vec{x}^{(k,i)}\right\|^2 + \lambda(\vec{a}_i^T \vec{x} - y) \quad (12)$$

where λ is the Lagrange multiplier, which is also called the dual variable. The dual problem corresponding to Eq. (12) is defined below.

$$\max_{\lambda} D(\lambda) \equiv \min_{(\vec{x},y)} L(\vec{x},y,\lambda) \ s.t. \lambda \in \Omega$$
$$\Omega = \{\lambda | D(\lambda) > -\infty\} \quad (13)$$

where $D(\lambda)$ is the dual function and Ω is the domain on which $D(\lambda)$ is defined. In the current case, the dual problem can be solved by the following steps.

First, minimization problem corresponding to variable y, *i.e.* solving Eq. (14).

$$\arg\min_{y} \|y - b_i\|^2 - \lambda y \quad (14)$$

The value y= $b_i + \lambda/2$ makes Eq. (14) take the minimum. Then substitute y by $b_i + \frac{1}{2}\lambda$ in $D(\lambda)$ and solve the next minimization problem corresponding to variable $\vec{x}$, *i.e.* solving Eq. (15).

$$\arg\min_{\vec{x}} \frac{1}{2\alpha^{(k)}} \left\|\vec{x} - \vec{x}^{(k,i)}\right\|^2 + \lambda \vec{a}_i^T \vec{x} \quad (15)$$

By solving Eq. (15), the iterative formula can be derived as below.

$$\vec{x} = \vec{x}^{(k,i)} - \lambda \alpha^{(k)} \vec{a}_i \quad (16)$$

Finally, substitute $\vec{x}$ by Eq. (16) in $D(\lambda)$ and obtain the maximization problem corresponding to variable λ as follows.

$$\max_{\lambda} D(\lambda) = \max_{\lambda} \left(-\frac{1}{4} - \frac{1}{2}\alpha^{(k)} \|\vec{a}_i\|_2^2 \right) \lambda^2 + (\vec{a}_i^T \vec{x}^{(k,i)} - b_i) \lambda \quad (17)$$

It is obvious that Eq. (17) is a quadratic function about λ, and it is easy to find the λ value which makes $D(\lambda)$ take the maximum. The update formula of λ is expressed as Eq. (18).

$$\lambda = -\frac{2(b_i - \vec{a}_i^T \vec{x}^{(k,i)})}{1 + 2\alpha^{(k)} \|\vec{a}_i\|_2^2} \quad (18)$$

So far, we have already obtained the complete iteration formula as follows for the accelerated SIRT algorithm.

$$\lambda = -\frac{2(b_i - \vec{a}_i^T \vec{x}^{(k,i)})}{1 + 2\alpha^{(k)} \|\vec{a}_i\|_2^2}, \quad \vec{x}^{(k,i+1)} = \vec{x}^{(k,i)} - \lambda \alpha^{(k)} \vec{a}_i \quad (19)$$

With respect to the selection of step-size parameter $\alpha^{(k)}$, we use a diminishing step-size rule expressed as

$$\alpha^{(k)} = \frac{\alpha_0}{1 + \varepsilon K} \quad (20)$$

where ($\alpha_0 > 0, \varepsilon > 0$) are pre-specified parameters in the step-size control stage. Eq. (19) possesses a row-action type structure similar to the ART algorithm, which guarantees the high convergence speed. In tomographic image reconstruction fields, there is a strong trend that people prefer such iterative algorithms, because they can be implemented easily thanks to the necessity of accessing only a single row of system matrix A for each image update. Furthermore, it is known that such algorithms can be made computationally efficient by using the special data access order described by Herman and Meyer [3]. We used this data access order in our implementations. The proposed accelerated SIRT algorithm is shown in Table I.

Table I. The proposed accelerated SIRT algorithm

Initialization: Set $\vec{x}^{(0,1)} \rightarrow 0$. Give the initial value of step-size control parameters ($\alpha_0 > 0$, $\varepsilon > 0$). Execute the following steps for k=0, 1, 2, ⋯.

Step 1: Calculate the step-size parameter $\alpha^{(k)}$, $\alpha^{(k)} = \frac{\alpha_0}{1 + \varepsilon K}$.

Step 2: Execute the following steps for i=1, 2, ⋯, I.

(2.1) Compute λ: $\lambda = -\frac{2(b_i - \vec{a}_i^T \vec{x}^{(k,i)})}{1 + 2\alpha^{(k)} \|\vec{a}_i\|_2^2}$

(2.2) Update $\vec{x}$: $\vec{x}^{(k,i+1)} = \vec{x}^{(k,i)} - \lambda\alpha^{(k)}\vec{a}_i$

Step 3: $\vec{x}^{(k+1,1)} = \vec{x}^{(k,I+1)}$

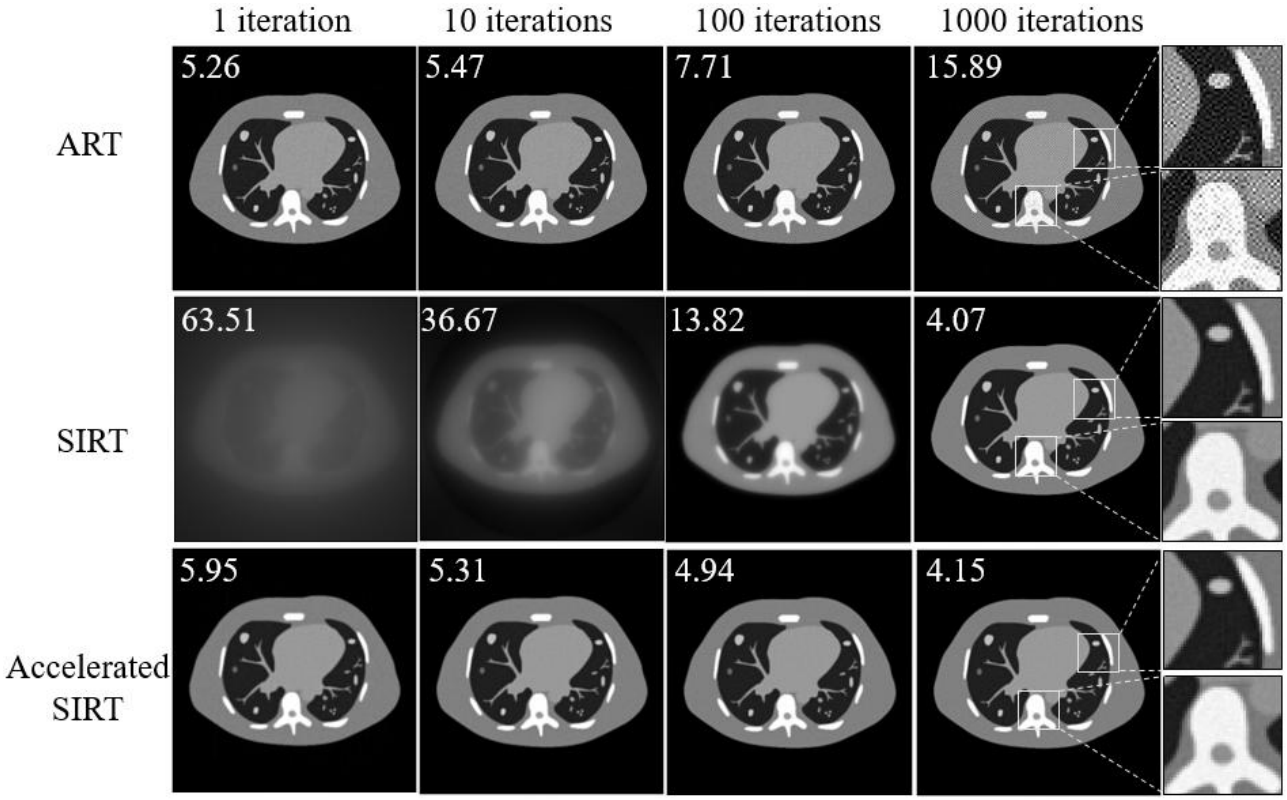

Figure 2. Reconstructed images by the conventional ART, SIRT and the proposed accelerated SIRT algorithms. Reconstructed images corresponding to 1, 10, 100 and 1000 iterations are shown.

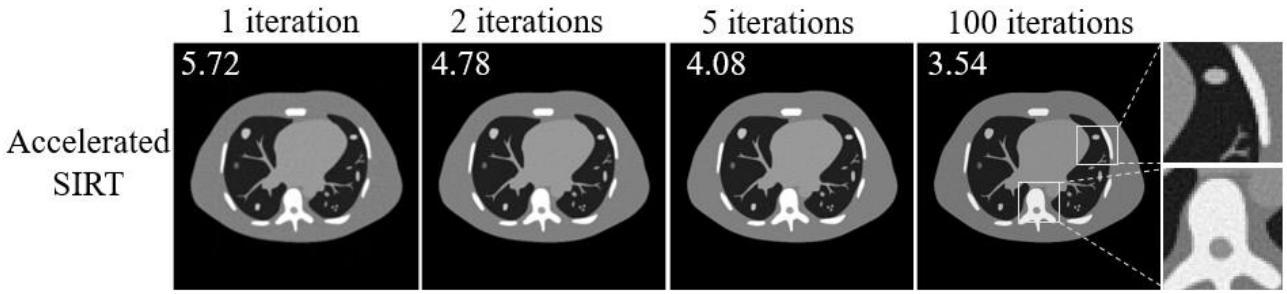

Figure 3. Reconstructed images of numerical chest phantom by the modified accelerated SIRT algorithm. Reconstructed images corresponding to 1, 2, 5 and 100 iterations are shown.

Some readers may concern about the convergence property. Because in Passty's theorem, only the ergodic average of the iterates $\vec{x}^{(k',\,I+1)}$ ($k' = 0, 1, 2, \cdots, k$) was proved to be convergent. We show Passty's theorem below.

[**Theorem**] Define ergodic average of the iterates $\vec{x}^{(k',\,I+1)}$ by

$$\bar{\vec{x}}^{(k)} = \frac{\sum_{k'=0}^{k} \alpha^{(k')}\vec{x}^{(k',\,I+1)}}{\sum_{k'=0}^{k} \alpha^{(k')}} \tag{21}$$

Then, $\bar{\vec{x}}^{(k)}$ converges to a minimizer of $F(\vec{x})$ when the diminishing step-size rule is satisfied.

We note that the above convergence is called the ergodic convergence, which is more credible than the convergence of sequence $\vec{x}^{(k,I+1)}$ itself to a minimizer of $F(\vec{x})$. In order to simplify the implementation of above ergodic convergence, a modified processing called oblivion procedure was proposed. This trick differs from Passty's theorem because it throws away the early stage iterates as the iteration goes on by adding a proper weight to each iterate. The procedure is expressed below.

$$\vec{s}^{(0)} = \alpha^{(0)}\vec{x}^{(0)}, \vec{s}^{(k)} = \theta\vec{s}^{(k-1)} + (1-\theta)\alpha^{(k)}\vec{x}^{(k)} \quad 0 < \theta < 1$$
$$\omega^{(0)} = \alpha^{(0)}, \omega^{(k)} = \theta\omega^{(k-1)} + (1-\theta)\alpha^{(k)} \quad 0 < \theta < 1$$
$$\vec{u}^{(k)} = \frac{\vec{s}^{(k)}}{\omega^{(k)}} \tag{22}$$

The weighted average $\vec{u}^{(k)}$ possesses the characteristic of losing the early stage iterates, but it can lead to a fast and mathematically accurate convergence. This is a good choice for

readers who care about the rigorous convergence when using proximal splitting framework. In practice, however, we have never observed a situation in which the ergodic convergence occurs but the sequence $\vec{x}^{(k,I+1)}$ itself is not convergent. Therefore, we conjecture that the proposed algorithm can be used without being anxious about the non-convergence.

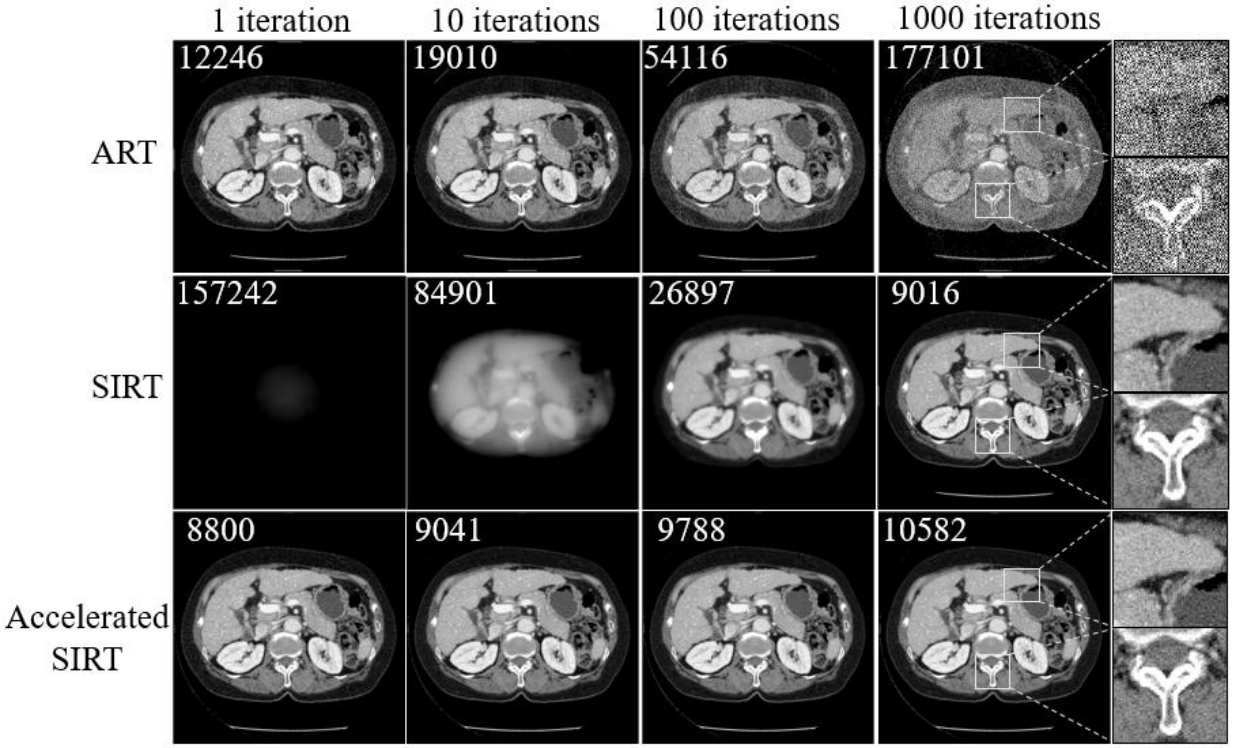

Figure 4. Reconstructed images of practical abdominal CT slice by ART, SIRT and accelerated SIRT algorithms. Reconstructed images corresponding to 1, 10, 100 and 1000 iterations are shown.

3.3 More on Step-size Control Parameter

In this paper, we furtherly emploied an additional modification to accelerate the convergence speed for the new algorithm. We discovered that, even in one cycle of the main iteration, the noise propagation from projection data to the reconstructed image is substantially independent of the access order of projection factors (subsets). Namely, the early stage reconstructed images are nearly free from noise affection, and they show relatively high image quality. However, the images reconstructed by the later subsets are vulnerable to noise. In order to adjust the balance of noise propagation among a single main iteration, it is advisable to set a bigger step-size value for the early stage reconstructions which use the former subsets, and let the step-size value be diminishing as the reconstruction goes on. Therefore, we introduced a subset-dependent (dynamic) step-size control parameter which is expressed below.

$$\alpha_k(q) = \frac{\alpha_0 \cdot \beta_0}{\beta_0 + q + \mu \cdot k \cdot M} \tag{23}$$

In Eq. (23), the symbol α_0 , β_0 and μ are pre-specified constant values, M represents the number of projection data factors which equals to I, q ($0 \le q \le M-1$) is the access order of the projection data, and k denotes the main iteration number. The new step-size controller makes step-size $\alpha_k(q)$ monotonically decreases along with the increasing q in a single main iteration. The idea was first proposed by Tanaka for image reconstruction of positron emission tomography [14]. We introduced this idea and combined it with the aforementioned proximal splitting. The combination furtherly accelerated the convergence speed, which became another novelty point of this paper.

4. EXPERIMENTAL RESULTS AND ANALYSIS

4.1 Numerical Phantom Reconstruction

In this simulation, we implemented the conventional ART algorithm, SIRT algorithm, and the proposed accelerated SIRT algorithm for comparison. The numerical chest phantom containing cardiac organ, bronchus, blood vessels, and vertebral column parts was designed for this comparison. The image size was 256 × 256 pixels and the projection data was acquired by parallel-beam geometry with 256 radial bins and 256 views over 180° angular range. In order to test the ability of reducing statistical noise in reconstructed images, we added Poisson noise in acquired projection data. The amount of photons which produce Poisson noise was 5.0e5. For the SIRT algorithm, the step-size parameter was set as $\alpha = 0.002$. For the accelerated SIRT algorithm, the step-size control parameters α_0 and ε were set as $\alpha_0 = 0.003, \varepsilon = 20$. The iteration number k was set to 1000. With respect to the image quality evaluation, we utilized a quantitative evaluating metric called root mean squared error (RMSE) which is commonly used as quality assessment for medical image reconstruction. It indicates the difference between the reconstructed image and the ground truth image. The RMSE value is calculated using Eq. (24).

$$\mathrm{RMSE}(\vec{x}) = \sqrt{\sum_{j=1}^{J} (x_j - x_j^{'})^2 \Big/ \sum_{j=1}^{J} 1} \tag{24}$$

where x_j denotes the pixel value of reconstructed image, and $x_j^{'}$ denotes the pixel value of ground truth.

The reconstruction results are shown in Figure. 2. In order to provide an accurate observation, we made a zoomed-up version for two parts of the 1000 iteration image, and listed them next to their host image. The results show that the ART algorithm and the proposed accelerated SIRT algorithm converged rapidly and they can obtain an ideal image structure in less than 10 iterations. However, the SIRT algorithm needed much more iterations until convergence. With respect to the noise depression effect, the SIRT and accelerated SIRT methods showed the superiority in noise reduction, and they depicted clear organ structures and image textures. But the result images reconstructed by ART were contaminated by noise, in which the noise was additionally obvious in zoomed-up images. We calculated the RMSE values for corresponding result images and presented them in the top left corner of each result image. The RMSE values revealed the same effect as visual evaluation. The SIRT and accelerated SIRT achieved much smaller RMSE value than that of ART, which showed their outstanding denoising effect. Besides, we recorded the implementing time for each method. 937s was needed for SIRT until its convergence of 1000 iterations, but it took only 48s for accelerated SIRT until its convergence of 20 iterations. Accelerated ratio was surprisingly almost 20 times.

Next, we did the reconstruction experiment by accelerated SIRT using the modified step-size control parameter. Exploratory experiments revealed that the product of $\alpha_0 \cdot \beta_0$ related with situation of convergence and noise propagation. Namely, when the product of $\alpha_0 \cdot \beta_0$ is too big, it is difficult to guarantee its convergence and much noise will be remained in the reconstructed image. On the contrary, too small $\alpha_0 \cdot \beta_0$ value can help removing noise well, but it will result in extremely slow convergence. Thus proper $\alpha_0 \cdot \beta_0$ value tuning is necessary. In our study, the optimal combination we found was $\alpha_0 = 1$, $\beta_0 = 100$. And other parameters were set as $\mu = 1$, M=256 × 256, q looped from 0 to M-1. Figure. 3 showed the reconstructed images corresponding to 1, 2, 5 and 100 iterations. It is obvious that the modified step-size succeed in achieving faster convergence and higher image quality. The RMSE value of the 2_{nd} iteration has defeated the value of the 100_{th} iteration of the original accelerated SIRT. Additionally, the result image converged to a smaller RMSE value.

4.2 Actual CT Image Reconstruction

A slice of upper abdominal CT image was used for reconstruction to test the efficiency of the proposed algorithm. The image size is 512 × 512, and projection data was acquired with 512 views over 180 ° angular range. Pixel spacing is 0.625mm, thus the scanning range was 32cm × 32cm. Poisson noise was added in projection data and photons amount was 5.0e7. For SIRT, the step-size was set as $\alpha = 0.002$. For accelerated SIRT, $\alpha_0 = 0.003, \varepsilon = 20$. The iteration number k was set to 1000. The reconstruction results are shown in Figure. 4. Similarly, we presented the zoomed-up image parts and corresponding RMSE values. Similar to the numerical phantom instance, we observed that ART and accelerated SIRT had a high convergence speed, and that SIRT and accelerated SIRT had an excellent noise reduction effect. The RMSE value was demonstrated in the top left corner of corresponding result images. It can be seen that the SIRT algorithm had a monotonic convergence, but ART and accelerated SIRT showed some vibration in convergence. But the accelerated SIRT obtained small enough RMSE value even in early iterations. Organ structures and image textures in the reconstructed image of ART were almost covered by noise. And SIRT and accelerated SIRT provided the clinically feasible image quality.

5. CONCLUSIONS

In this paper, we proposed an accelerated algorithm for the classical SIRT algorithm in the application of CT image reconstruction. The acceleration was achieved by applying Passty's proximal splitting framework, thus row-action type implementation structure was constructed successfully. This novel algorithm possesses the advantages of both classical ART and SIRT algorithms. Namely, the proposed algorithm not only has an excellent noise reducing ability, but also has a high convergence speed. The accelerated ratio can be almost up to 20 times. Both numerical phantom and practical CT image were reconstructed for the effect validation.

6. ACKNOWLEDGMENTS

This work was supported by JST-ERATO Project (Grant No. JPMJER1403), JST-CREST Project (Grant No. JPMJCR1765), and Natural Science Foundation of Tianjin City Project (No.18JCYBJC43600) and Tianjin Overseas Returnees Research Funding Support Project (No. 201819).

7. REFERENCES

[1] Herman GT. 2009. Fundamentals of computerized tomography: Image reconstruction from projections. *Springer Publications*.

[2] Radon J. 1986. On the determination of functions from their integral values along certain manifolds. *IEEE Trans Med Imaging*. Vol. 5, 170-176.

[3] Herman GT, Meyer LB. 1993. Algebraic reconstruction techniques can be made computationally efficient. *IEEE Trans Med Imaging*. Vol. 12, 600-609.

[4] Vasin VV, Eremin II. 2009. Operators and iterative processes of Fejer type. Walter de Gruyter.

[5] Y Kim, H Kudo, K Chigita, S Lian. 2019. Image reconstruction in sparse-view CT using improved nonlocal total variation regularization. *Proc. SPIE 11113.*

[6] H. Kudo. 2012. Image reconstruction of iterative algorithms (in Japanese). *The handbook of The Japanese Society of Medical Imaging Technology*. 55-60.

[7] P Despres, X Jia. 2017. A review of GPU-based medical image reconstruction. *Physica Medica.* Vol. 42, 76-92.

[8] J Dong, H Kudo, EA. Rashed. 2017. Compressed sensing of sparsity-constrained total variation minimization for CT image reconstruction. *Proc. SPIE Medic Imag*. Vol. 10132.

[9] KH. Jin, MT. McCann, E. Froustey, M. Unser. 2017. Deep convolution neural network for inverse problems in imaging. *IEEE Transactions on Image Processing*. Vol.26, No.9, 4509-4522.

[10] Y. Han, JC Ye. 2018. Framing U-Net via deep convolutional framelets: application to sparse-view CT. *IEEE Trans on Imag Proces*. Vol.37, No.6, 1418-1429.

[11] PL. Commettes, JC. Pesquet. 2010. Proximal splitting method in signal processing. *Fixed Point Algorithms for Inverse Problems in Science and Engineering*.

[12] Byrne CL. 2007. Applied iterative methods. *AK Peters Ltd Publication*.

[13] D.P.Bertsekas. 1999. Nonlinear programming. *Athena Scientific Publication*.

[14] E Tanaka, H Kudo. 2003. Subset-dependent relaxation in block-iterative algorithms for image reconstruction in emission tomography. *Physics in Medicine and Biology*. Vol.48, No.10, 1405-1422.